Paper No. 414. (quote when citing this article)
Eleventh World Conference on Earthquake Engineering
ISBN: 0 08 042822 3

ULTIMATE STRENGTH AND PLASTIC DEFORMATION CAPCITY OF CFT BEAM-COLUMN SUBJECTED TO DYNAMIC LOAD

KAZUAKI MITSUNARI[1] and MOTOO SAISHO[2]

[1] Arai-Gumi Ltd.,
Nishinomiya, Hyogo 662, Japan

[2] Department of Architecture, Kumamoto University,
Kurokami 2-39-1, Kumamoto 860, Japan

ABSTRACT

In order to make the practical use of super-high strength concrete in earthquake resistant design, dynamic loading test of high strength concrete filled steel tube (HCFT) is carried out. From the test results of ultimate strength and plastic deformation capacity it is confirmed that HCFT beam-column is useful in earthquake resistant design of building structures. But it is also shown that the ultimate behavior and the ultimate strength of HCFT beam-column are quite different from these of CFT beam-column filled with widely-used concrete because of the brittle fracture and the confined effect of filled concrete. Accordingly the confined concrete strength (σ_{ce}) is derived basing on stub column test. Using σ_{ce}, the modified superposed method of strength is proposed which can predict uniformly the ultimate strength of CFT beam-column filled with not only widely used concrete but also super-high strength concrete.

KEYWORDS

concrete filled steel tube, high-strength concrete, stub-column, beam-column, dynamic loading test, ultimate strength, crack development of steel tube, brittle fracture, loading rate effect

1. INTRODUCTION

Super-high strength concrete can be produced comparatively easily by the use of super-plasticizer and silica fume. It is expected by many designers of structure to make the practical use of super-high strength concrete to improve the design possibility of building structure. In earthquake resistant design, concrete filled steel tube (CFT) is considered to be suitable to use super-high strength concrete.

On the other hand it is well known that the high strength structural material is generally brittle. Furthermore it is well known that super-high strength concrete fractures in brittle due to the loading rate effect when it is subjected to dynamic load like seismic load. [2)-4)]

In earthquake resistant design against strong ground motion, the brittle fracture of structural member may be a cause to collapse the whole structure and to decrease extremely the earthquake resistant capacity of structure. From the reasons mentioned above, the fracture and ultimate strength of super-high strength concrete filled steel tube (HCFT) under dynamic load are investigated experimentally in this study in relation with the strength of filled concrete.

2. MATERIAL PROPERTIES OF SPECIMENS

CFT stub-column test and CFT beam-column test are carried out in this paper. In the specimens of these tests three kind of concrete and three kinds of steel tube are used. The three kinds of steel tube are cold-formed circular steel tube whose diameter-thickness ratio are approximately 30, 50 and 60. In Table 1 there are the material properties of them. The three kinds of filled concrete are super-high strength concrete (S), high strength concrete (H) and widely used concrete (L) whose mix proportions are explained in Table 2. The material properties of them are in Table 3-4.

3. STUB-COLUMN TEST

Specimens and test conditions

To investigate the confined effect of CFT member in relation with the filled concrete strength, stub-column test was carried out. Specimens and results of stub-column test are shown in Table 3. The stub-column test was executed under the condition that the aspect ratio(L/D) of every specimen is the same (L/D=3). The loading conditions and the measuring devices are explained in Fig.1.

ECS and ESS of stub-column

The stress-strain relations of steel tube are the round-house type as shown in Fig.2. The stress and strain in Fig.2 are normalized by σ_u (σ_u: ultimate stress) and ε_p ($=\sigma_u/E$, E: modulus of elasticity). As we can see, they are approximated by the bi-linear model which is drawn by dashed line in it. According to the relation between the axial strain (ε_A) and the lateral strain (ε_L) of steel tube which is shown in Fig.3, they are approximately expressed by Eq.(1)

$$\varepsilon_A = -\varepsilon_L \qquad (1)$$

Applying the conditions mentioned above to the Tresca's yield condition, the steel tube stress of CFT stub column is given by the point "P" in Fig.4 and expressed by Eq.(2).

$$\sigma_A = -\sigma_u/2$$
$$\sigma_L = \sigma_u/2 \qquad (2)$$

in which σ_A, σ_L: the axial stress and tangential stress of steel tube.

From Eq.(2) the equivalent axial stress of steel tube of

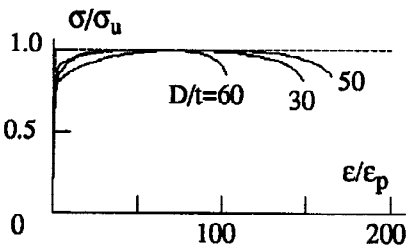

Fig.2 Stress-strain relation of steel tube and its bi-linear model

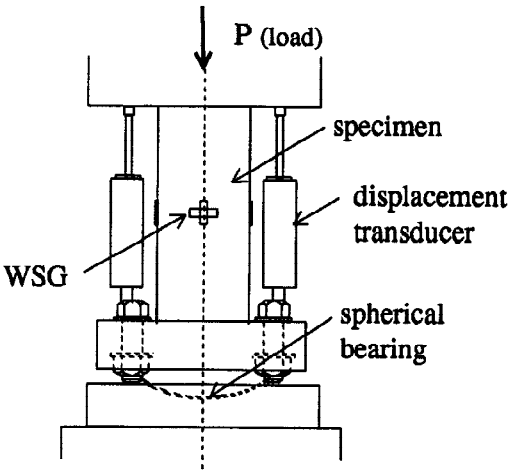

Fig.1 Test setup of CFT stub-column test

Table 1 Material properties of steel tube

steel tube	tensile test (tf/cm²) σ_y	(tf/cm²) σ_u	(%) ε_u	stub column test (tf/cm²) ${}_c\sigma_y$	(tf/cm²) ${}_c\sigma_u$	(%) ${}_c\varepsilon_u$
φ-101.6x3.2	3.85	4.64	23.8	3.77	4.27	2.05
φ-139.8x2.8	3.48	4.52	28.8	3.34	3.60	0.86
φ-139.8x2.4	4.72	5.60	22.6	4.38	4.74	0.79

σ_y, ${}_c\sigma_y$: yield stress, σ_u, ${}_c\sigma_u$: maximum stress , ε_u, ${}_c\varepsilon_u$: strain at σ_u, ${}_c\sigma_u$

Table 2 Mix proportion of filled concrete (oven-dry state)

concrete	W/C (%)	mix proportion(kgf/m³) water	cement	silica fume	aggregate FA	aggregate CA	admixture
Super-high strength concrete (S)	20	150	625	125	568	1010	22
High strength concrete (H)	35	194	555	-	613	1094	7
Widely used concrete (L)	60	216	360	-	762	1063	-

FA :weight of fine aggregate per unit volume of concrete
CA :weight of coarse aggregate per unit volume of concrete

CFT stub-column (ESS), which is effected by confining the filled concrete, is given by "$-\sigma_u/2$".
Considering the equilibrium condition in axial direction of CFT stub-column, the equivalent concrete strength (ECS), which is effected by being confined by steel tube, is given by Eq.(3)

$$\sigma_{ce} = (P_{max} - A_s \sigma_u/2)/A_c \qquad (3)$$

in which P_{max}: the maximum load of stub-column test, A_s, A_c: sectional areas of steel tube and filled concrete respectively.
The derived values of ECS (σ_{ce}) are plotted in Fig.5 in which $\xi(=\sigma_u A_s/\sigma_c A_c)$ means the strength ratio of steel tube to filled concrete. As shown in Fig.5 by the dashed line, the values of σ_{ce} can be fairly approximated by Eq.(4).

$$\sigma_{ce}/\sigma_c = 0.69\xi + 0.81 \qquad (4)$$

In Fig.5, many stub-column test results which have been reported [4] are also plotted and compared with Eq.(4).

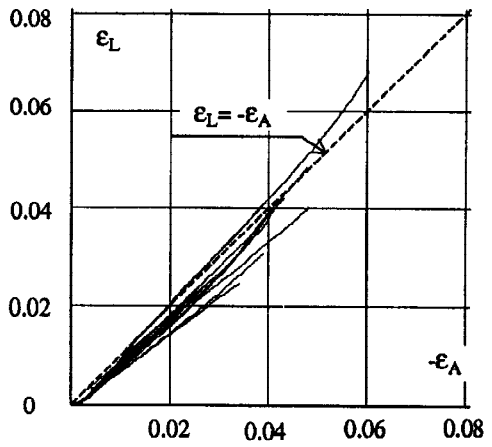

Fig.3 Relation between axial strain (ε_A) and lateral strain (ε_L) of steel tube

Table 3 Stub-column specimens and test results

Specimen	D (mm)	t (mm)	D/t	σ_c (kgf/cm²)	ε_c (%)	ξ	N_y (tf)	N_u (tf)	P_{max} (tf)	σ_{ce}/σ_c
S-30.1	101.4	3.0	34	1194	0.36	0.50	121	128	114	1.08
S-30.2	〃	〃	〃	〃	〃	〃	〃	〃	122	1.18
S-30.3	101.5	〃	〃	1384	0.35	0.43	135	142	121	1.00
S-50.1	139.9	2.8	50	1194	0.36	0.32	211	224	211	1.08
S-50.2	〃	〃	〃	〃	〃	〃	〃	〃	200	1.02
S-50.3	〃	〃	〃	1384	0.35	0.28	238	250	213	0.95
S-50.4	140.0	〃	〃	〃	〃	〃	〃	〃	209	0.93
S-50.5	139.9	〃	〃	〃	〃	〃	〃	〃	212	0.94
S-60.1	139.8	2.4	59	1384	0.34	0.29	247	256	222	0.98
S-60.2	〃	〃	〃	〃	〃	〃	〃	〃	218	0.95
H-30.1	101.5	3.0	34	637	0.24	0.93	81	88	94	1.60
H-30.2	〃	〃	〃	〃	〃	〃	〃	〃	〃	〃
H-30.3	〃	〃	〃	〃	〃	〃	〃	〃	92	1.55
H-50.1	139.9	2.8	50	585	0.23	0.66	125	137	135	1.30
H-50.2	〃	〃	〃	〃	〃	〃	〃	〃	142	1.39
H-50.3	〃	〃	〃	〃	〃	〃	〃	〃	134	1.29
H-60.1	140.0	2.4	59	637	0.24	0.63	140	149	159	1.43
H-60.2	139.8	〃	〃	724	0.34	0.55	152	161	161	1.28
H-60.3	139.7	〃	〃	〃	〃	〃	〃	〃	〃	〃
L-30.1	101.6	3.0	34	259	0.20	2.29	54	61	69	2.54
L-30.2	101.5	〃	〃	283	〃	2.10	56	63	73	2.72
L-30.3	〃	〃	〃	300	〃	1.98	57	64	73	2.73
L-50.1	139.9	2.8	50	259	〃	1.48	79	91	95	1.82
L-50.2	〃	〃	〃	283	〃	〃	〃	〃	97	1.88
L-60.1	139.8	2.4	59	〃	0.20	1.41	89	98	112	2.21
L-60.2	139.9	〃	〃	〃	〃	〃	〃	〃	113	2.22

D: diameter of steel tube, t : thickness of steel tube, σ_c: concrete strength, ε_c: concrete strain at σ_c, N_y: yield axial force, N_u: ultimate axial force, P_{max} :the maximum load, σ_{ce}: confined concrete strength, $\xi(=\sigma_u As/\sigma_c Ac)$:strength ratio of steel tube to infilled concrete

4. BEAM-COLUMN TEST

Specimens

In order to test on CFT beam-column of rigid frame, every specimen is designed as the cross-formed type composed of CFT column and H-steel beams. (Fig.6) The mechanical properties of circular steel tube and filled concrete of specimen are explained in Table 4. The concrete strength, diameter-thickness ratio of steel tube, axial load, loading rate and forced deformation of these specimens are varied among them.

Loading conditions and measurements

Loading condition of test is explained in Fig.7 and test setup is shown in Fig.8. Constant axial force (N) and alternating repeated lateral force (F) were loaded at the column end through an universal joint. The constant axial load (N), whose values are in Table.4, was loaded using the weight based on the lever-principle. (Fig.8) The time histories of forced deformation at the loading point (Df) in dynamic loading test are expressed in Fig.9. They are the irregular wave obtained from seismic response displacement (R) and the sinusoidal waves whose amplitude are constant (C) and gradually increasing (I). The maximum velocity of deformation was about 10cm/sec. and the maximum strain rate, which was obtained by wire strain gages attached to the surface of steel tube 3cm apart from the column end, was 0.1/sec.-0.3/sec.

To investigate the effect of loading rate, static loading tests were also carried out in addition to the dynamic loading test. In static test the hysteretic deformation at the loading point (Df) is the same as the dynamic loading test. The load was given in step-by-step in static test. After small incremental deformation is given, the forced deformation was kept constant in one minute in every incremental step to complete the enough stress relaxation and exclude the effect of loading rate and then the load, displacements and strains were measured at the same time.

Restoring force characteristics

In Fig.10 there are the load-deformation relationships of test result. The load (Mc) in this figure is the column end-moment including P-Δ effect of axial force and the deformation (Dc) is the of column deflection as

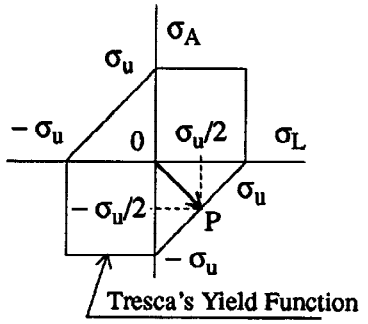

Fig.4 The yield condition and stress hysteresis in steel tube

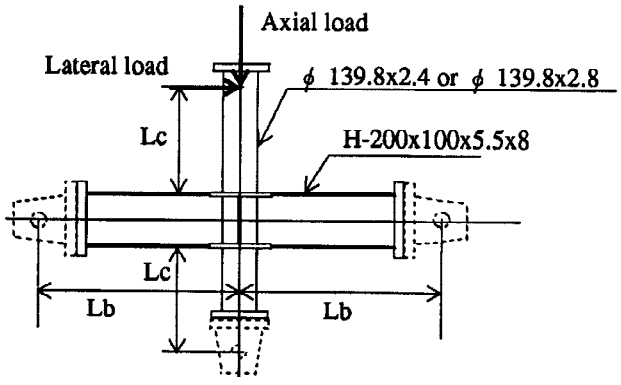

Fig.6 CFT beam-column specimen

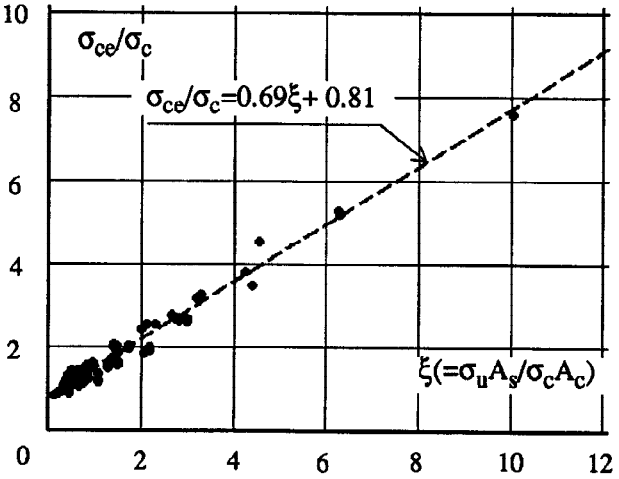

Fig.5 Confined concrete strength (σ_{ce}) of CFT stub column

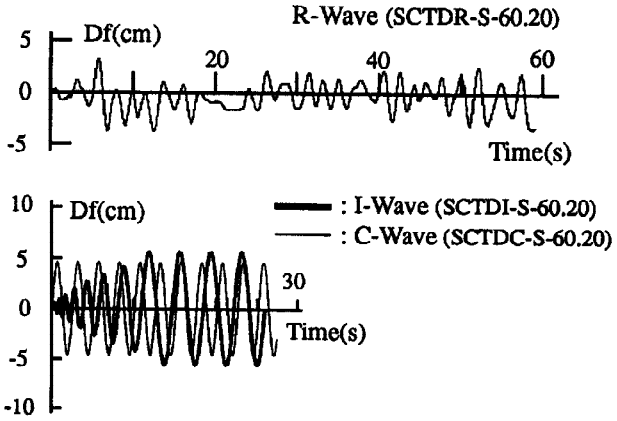

Fig.9 Time histories of forced displacement (Df)

explained in Fig.7.
It is shown in this figure that the restoring force and ultimate strength of CFT beam-column increases clearly as the filled concrete strength increases. Every specimen also shows the excellent plastic deformation capacity and energy absorbing capacity as beam-column of earthquake resistant structure.

Ultimate state of CFT beam-column
Concerning with the ultimate behavior of CFT beam--column under constant axial load and repeated lateral load, there are the following two types.

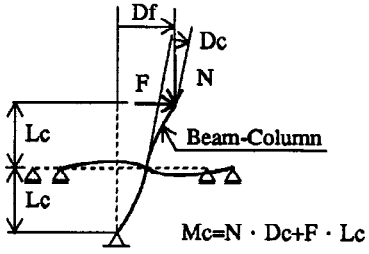

Fig.7 Loading condition

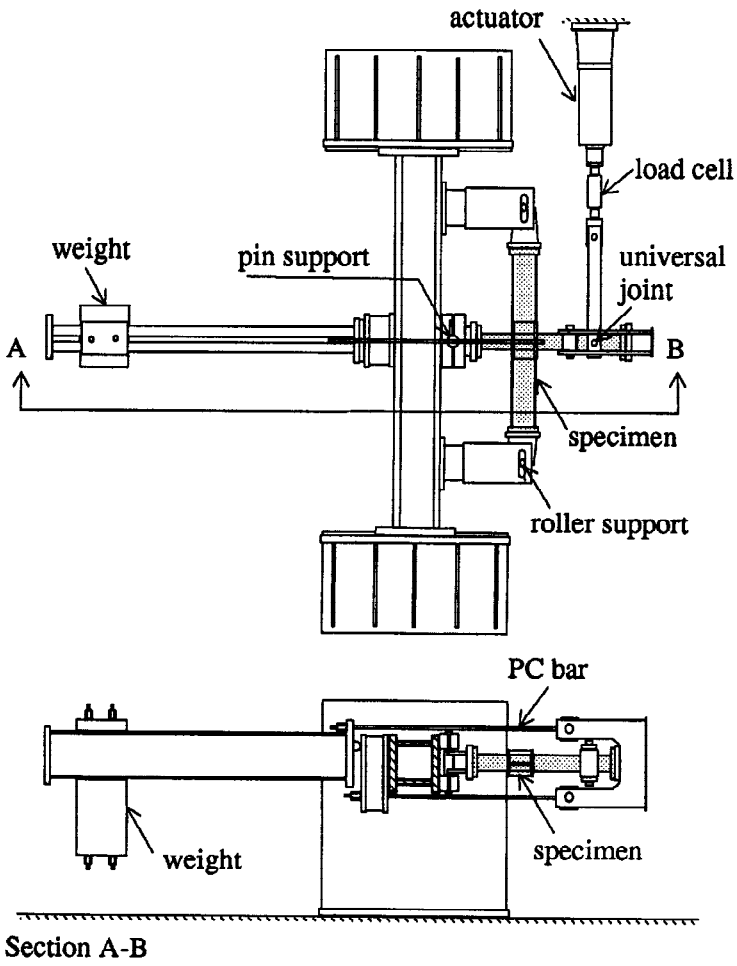

Fig.8 Test setup of CFT beam-column test

i) Axial deformation increases gradually by accumulating plastic deformation and finally the specimen can not bear the constant axial load. (Fig.13) This ultimate state of test is expressed by "AX" in Table 4.

ii) Steel tube crack develops near the column end and the steel tube is fully cut crosswise at the section. When the steel tube crack develops, the restoring force of CFT beam-column degrades drastically. The ultimate state of crack development is expressed by "CR" in Table 4.
In the ultimate state of AX, there is not remarkable degrading of restoring force. (Fig.12) On the other hand, in the ultimate state of CR, the restoring force of CFT beam-column degrades drastically and the fracture induced by the crack in steel tube is extremely brittle. In spite of the excellent plastic deformation capacity of CFT beam-column, we need to pay attention to the crack development behavior because the brittle fracture of

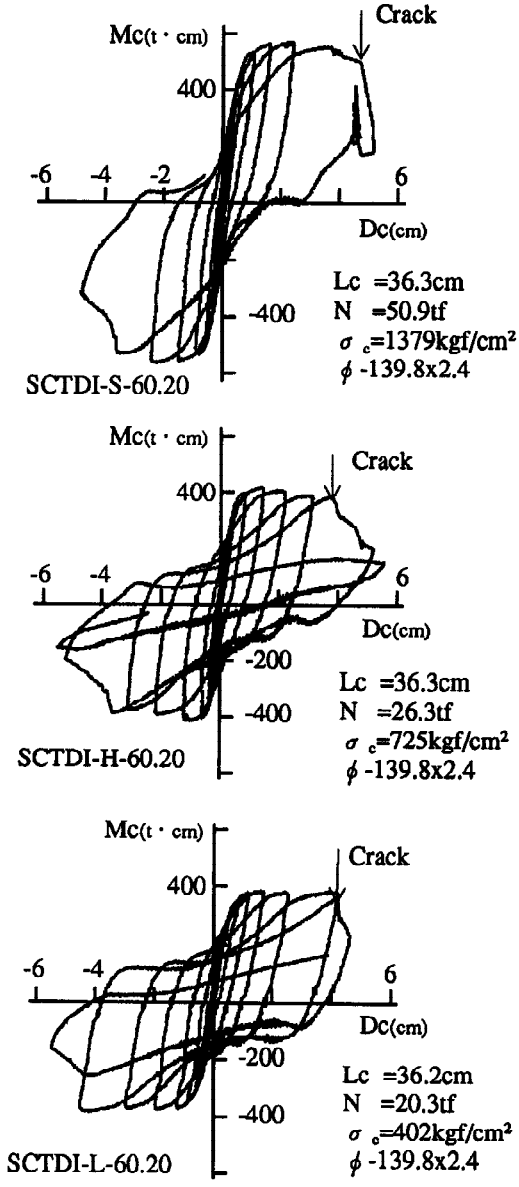

Fig.10 Load-deformation relations of dynamic loading test

beam-column is dangerous behavior in earthquake resistant design.

Loading rate effect

Load-deformation relationship of dynamic test is compared with that of static test in Fig.11. It is clear that the loading rate effect increases the restoring force and the ultimate strength of CFT beam-column. The loading rate effects of all specimens are summarized in Fig.14 by comparing the ultimate strength of dynamic test with that of static test. But the crack in steel tube developed earlier in dynamic test than static test. Accordingly the loading rate effect works to accelerate the crack development of steel tube and to decrease the ductility of CFT beam-column.

5. ULTIMATE STRENGTH OF CFT BEAM-COLUMN

The ultimate strengths obtained in CFT beam-column test are shown in Table 4 in which M_m is the maximum value of M_c.

In this chapter the values of M_m are compared with the ultimate strength (M_u) calculated by the widely used method of superposed strength. After that, a modified method to predict M_m is proposed.

Fig.14 shows the ratio of M_m to M_u which is expressed by the symbols of "○". We can see clearly the value of M_m/M_u decreases as the value of $1/\xi$ increases. In this figure, M_u is calculated by the method of superposed strength using the yield stress of steel (σ_y) and the compression strength of concrete (σ_c). Namely M_u is the full plastic moment defined by σ_y and σ_c. Especially we need to pay attention to M_m/M_u values of the super-high strength concrete filled steel tube which are smaller than those of low strength concrete filled steel tube. From this reason, the widely used method of superposed strength can not be applied simply to any kind of CFT beam-columns. The reason why the value of M_m/M_u changes according to the concrete strength is that the confined effect is neglected in the calculation by the superposed strength method.

The confined effect of concrete has derived based on the stub-column test and expressed by Eq.(4). Using the confined concrete strength (σ_{ce}) given by Eq.(4), the ultimate strengths of CFT beam-column (M_{ue}) are obtained by the superposed strength method and compared with the test results (M_m). They are drawn by the symbols of "●" in Fig.14. In this calculation it is assumed that the confined concrete strength of CFT beam-column under constant axial load and repeated lateral load can be given by the confined concrete strength of stub-column test (σ_{ce}) expressed by Eq.(4). It is also assumed that the stress of steel tube of CFT beam-column can be given by the ultimate stress (σ_u) defined by the bi-linear model in Fig.2 because of the cyclic hardening of steel tube.

As shown in Fig.14, there is not clear difference of $M_m/$

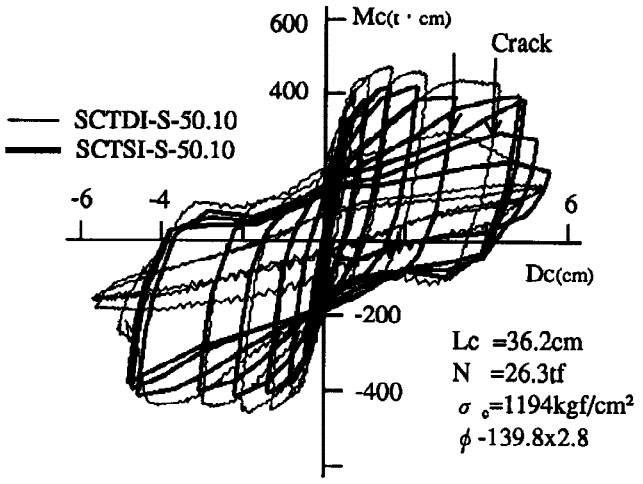

Fig.11 Load-deformation relations of dynamic loading test (SCTDI-S-50.10) and static loading test (SCTSI-S-50.10)

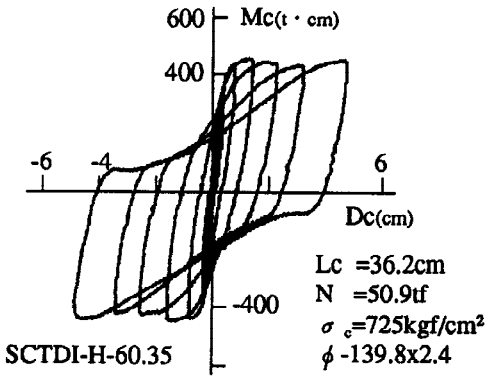

Fig.12 Load-deformation relation of SCTDI-H-60.35 whose plastic axial deformation was accumulated extremely

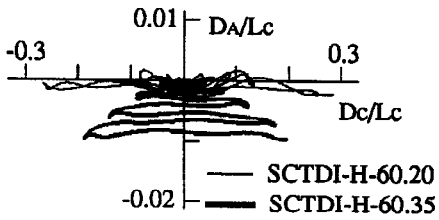

Fig.13 Axial deformations (D_A) with accumulated plastic deformation (SCTDI-H-60.35) and without accumulation (SCTDI-H-60.20)

Table 4 Beam-column specimens and test results

Specimen	Section (steel tube)	Load	Def.	N/N_u	(cm) L_c	D/t	(t/cm^2) σ_c	$1/\xi$	Ultimate state	(t.cm) M_m
SCTDI-S-60.20	φ139.8x2.4	D	I	0.198	36.3	58.1	1.379	3.40	CR	571
SCTDI-S-60.10	"	"	"	0.103	"	"	"	"	CR	480
SCTDI-H-60.35	"	"	"	0.312	36.2	57.7	0.725	1.77	AX	457
SCTDI-H-60.20	"	"	"	0.161	36.3	"	"	"	CR	419
SCTDI-L-60.45	"	"	"	0.438	36.2	57.9	0.402	0.99	AX	450
SCTDI-L-60.25	"	"	"	0.226	"	"	"	"	CR	402
SCTDI-L-60.20	"	"	"	0.174	36.3	"	"	"	CR	387
SCTDC-S-60.20	φ139.8x2.4	D	C	0.198	36.3	57.4	1.379	3.35	CR	590
SCTDC-S-60.10	"	"	"	0.102	"	"	"	"	CR	505
SCTDC-H-60.20	"	"	"	0.161	"	57.7	0.725	1.77	CR	428
SCTDC-L-60.45	"	"	"	0.450	36.2	57.9	0.402	0.99	AX	476
SCTDC-L-60.20	"	"	"	0.200	36.3	"	"	"	CR	419
SCTSC-S-60.20	φ139.8x2.4	S	C	0.198	36.3	57.4	1.379	3.35	CR	540
SCTSC-L-60.45	"	"	"	0.450	36.2	57.9	0.402	0.99	AX	419
SCTSC-L-60.20	"	"	"	0.200	"	"	"	"	CR	379
SCTDR-S-60.20	φ139.8x2.4	D	R	0.198	36.3	58.1	1.379	3.40	CR	566
SCTDR-L-60.20	"	"	"	0.200	36.2	57.9	0.402	0.99	CR	411
SCTDI-S-50.25	φ139.8x2.8	D	I	0.227	36.2	50.4	1.194	3.14	CR	529
SCTDI-S-50.10	"	"	"	0.117	36.3	"	"	"	CR	473
SCTDI-H-50.35	"	"	"	0.370	"	"	0.585	1.54	CR	481
SCTDI-H-50.20	"	"	"	0.191	36.2	"	"	"	CR	443
SCTDI-L-50.25	"	"	"	0.249	"	50.5	0.359	0.94	CR	395
SCTDI-L-50.45	"	"	"	0.450	"	50.4	0.302	0.79	AX	426
STDI -O-50.50	"	"	"	0.485	"	50.5	-	0.00	AX	191
SCTSI-S-50.25	φ139.8x2.8	S	I	0.227	36.2	50.4	1.194	3.14	CR	483
SCTSI-S-50.10	"	"	"	0.117	"	"	"	"	CR	422
SCTSI-H-50.35	"	"	"	0.370	36.3	"	0.585	1.54	AX	423
SCTSI-H-50.20	"	"	"	0.191	36.2	"	"	"	CR	395
SCTSI-L-50.25	"	"	"	0.249	"	50.5	0.359	0.94	CR	358
STSI -O-50.50	"	"	"	0.485	"	50.5	-	0.00	AX	150
SCTDC-H-50.25	φ139.8x2.8	D	C	0.250	36.2	50.4	0.724	1.90	CR	488
SCTDC-L-50.45	"	"	"	0.450	"	"	0.302	0.79	CR	409
SCTDC-L-50.25	"	"	"	0.250	"	"	"	0.79	CR	383
SCTDI-S-30.25	φ101.6x3.2	D	I	0.247	25.0	34.2	1.383	2.33	CR	302
SCTDI-S-30.10	"	"	"	0.108	24.9	"	1.308	2.20	CR	251
SCTDI-H-30.20	"	"	"	0.196	25.0	34.0	0.446	0.75	CR	225
SCTDI-L-30.25	"	"	"	0.264	"	"	0.180	0.30	CR	224
STDI -O-30.35	"	"	"	0.346	24.9	34.2	-	0.00	AX	141
SCTSI-S-30.25	φ101.6x3.2	S	I	0.248	25.0	34.2	1.383	2.33	CR	280
SCTSI-S-30.10	"	"	"	0.108	24.9	"	1.308	2.20	CR	233
SCTSI-H-30.20	"	"	"	0.197	"	34.0	0.446	0.75	CR	226
SCTSI-H-30.25	"	"	"	0.264	25.0	"	0.180	0.30	AX	-
STSI -O-30.35	"	"	"	0.346	24.9	34.2	-	0.00	AX	119
CTDI -S-30.25	φ101.6x3.2	D	I	0.253	50.2	34.2	1.336	2.25	CR	287
TDI -O-30.35	φ101.6x3.2	D	I	0.346	50.0	34.2	-	0.00	AX	126
TSI -O-30.35	"	S	"	0.345	"	34.3	-	0.00	AX	113
STDR-O-30.35	"	D	R	"	24.9	"	-	0.00	-	136
STSR-O-30.35	"	S	"	0.346	"	34.2	-	0.00	AX	123
TDR -O-30.35	"	D	"	"	50.0	"	-	0.00	-	131
TSR -O-30.35	"	S	"	0.345	50.1	34.3	-	0.00	-	124

D: dynamic load, S: static load, I,C,R: forced deformation types, N: axial load, $N_u=\sigma_c A_c+\sigma_u A_s$, L_c: column length, D/t: diameter-thickness ratio of steel tube, σ_c: concrete strength, $1/\xi=\sigma_c A_c/\sigma_u A_s$, CR,AX: types of ultimate state, M_m: ultimate strength of test

M_{ue} values according to the design condition (ξ) and the proposed method (M_{ue}) can predict the test values (M_m) fairly well compared with the widely used method (M_u).

6. CONCLUSIONS

Confined concrete strength (σ_{ce})

The confined concrete strength (σ_{ce}) of CFT stub-column can be approximated by Eq.(4) regardless of the filled concrete strength. (Fig.5)

Ultimate strength and fracture of HCFT beam-column

The restoring force and ultimate strength of CFT beam-column is increased as the strength of filled concrete and the loading rate increase. Simultaneously the increases of loading rate and concrete strength also work to accelerate the crack development of steel tube which is brittle fracture of CFT beam-column and decreases the restoring force of it drastically.

Prediction of the ultimate strength

When the ultimate strength of CFT beam-column test (M_m) is predicted by the widely used method of superposed strength (M_u), the value of M_m/M_u changes according to the design condition (ξ). From this result the method of superposed strength (M_u) can not simply used to deal with CFT beam-column of super-high strength concrete.

Using the confined concrete strength (σ_{ce}) and the ultimate stress of steel tube (σ_u), the modified superposed strength method is proposed to calculate the ultimate strength of CFT beam-column. This method can predict the ultimate strength of CFT beam-column uniformly regardless of the filled concrete strength even if it is the super-high strength concrete.

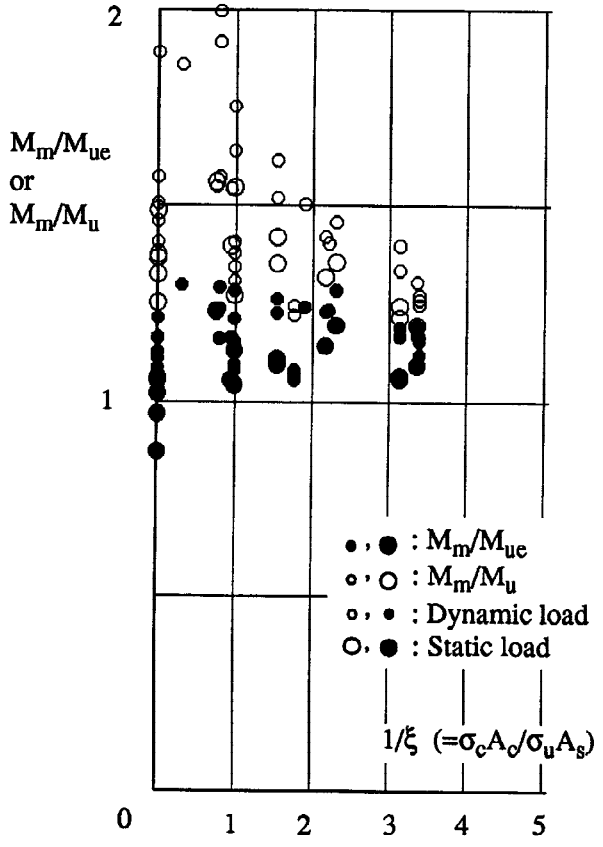

Fig.14 Comparison of predicted ultimate strengths (M_u, M_{ue}) with those of test result (M_m)

REFERENCES

1) Okamoto,T., Maeda,T., Masuo,K., Nishiyama,H. and Kaneta,K. (1995). Experimental study on the compressive strength of steel tube with high strength concrete using centrifugal compaction. *AIJ, 469*. 137-147. (in Japanese)

2) Saisho,M. and Mitsunari,K. (1992). Dynamic restoring force characteristics of steel tube filled with super-high strength concrete. *10-WCEE, VI*. 3201-3204.

3) Saisho,M. and Mitsunari,K. (1994). Experimental study on dynamic behavior of steel tube filled with super-high strength concrete. *4-ASCCS, Steel-composite structures*. 580-583.

4) Saisho,M., Okabe,T. and Mitsunari,K. (1996). Experimental study on confining effect and ultimate strength of high-strength concrete filled steel tube. *Journal of structural engineering, 40B*. (in Japanese)

ACKNOWLEGEMENT

The research reported here was supported by Sumitomo Metal Industries Ltd. and Tokai-Kogyo Ltd. Their financial support is gratefully acknowledged.